Theoretical and experimental study on the selectivity of dehydrogenation of α-limonene in ZSM-5 and zeolite-Y

P.A. Weyrich [a], W. Hölderich [a], M.A. van Daelen [b] and A.M. Gorman [b]

[a] *Department of Chemical Technology and Heterogeneous Catalysis, University of Technology, RWTH-Aachen, Worringerweg 1, D-52056, Aachen, Germany*
E-mail: hoelderich@rwth-aachen.de
[b] *Molecular Simulations, Inc., 9685 Scranton Road, San Diego, CA 92121, USA*

Received 16 December 1997; accepted 30 March 1998

Dehydrogenation of the natural terpene α-limonene to the industrially important p-cymene was studied over two zeolite-supported Pd catalysts, ZSM-5 and zeolite-Y. Reactor tests indicate that transalkylation of the p-cymene product can be avoided by employing the shape-selective properties of a medium-pore ZSM-5 catalyst. The diffusion properties of the three isomers of cymene were then calculated in the two zeolites using molecular mechanics. In case of ZSM-5, p-cymene was found to have the lowest barrier of the three isomers for diffusion through the straight, spherical channel of the zeolite. For zeolite-Y, differences in diffusivity for the three isomers were very small. Theory and experiments showed, in excellent agreement, that only ZSM-5 selectively produces p-cymene. This work shows that molecular mechanics is a powerful and reliable method for the screening of zeolites for performing shape-selective catalysis.

Keywords: selective hydrogenation, zeolite catalysis, forcefield simulations, biased diffusion method, ZSM-5 and zeolite-Y catalysts

1. Introduction

p-cymene is an important starting material for the production of many intermediates and end-products, such as p-cresol, fragrances, herbicides, pharmaceuticals, and heat transfer media [1,2]. Conventionally, cymenes are manufactured by Friedel–Crafts alkylation of toluene with propene using hazardous catalysts like $AlCl_3$ [3]. However, this process is non-selective and leads to cymene mixtures in thermodynamic equilibrium composition.

Recently, selective synthesis of p-cymene by zeolites has been thoroughly investigated [4–7]. Zeolite-based processes avoid (1) the disposal of spent catalyst, (2) product contamination by the catalyst, (3) separation of the catalyst from the product, and (4) corrosion of the reactor and tubes. However, the formation of undesired m-cymene and para-n-propyltoluene, in addition to p-cymene, is seen particularly on MFI-type zeolites (ZSM-5). Furthermore, the conversions obtained are very low (4–10%). In contrast, large-pore zeolites yield additionally significant amounts of m- and o-cymene as well as meta-n-propoyltoluene, besides p-cymene and meta-n-propyltoluene, respectively.

Alternative approaches to synthesize p-cymene selectively start from α-limonene, a material with a structure very similar to p-cymene. α-limonene is widely and cheaply available as a by-product in the production of orange and lemon juice and as a component of mixed terpene feedstocks of the paper and pulp industry.

Earlier studies [8,9] have shown that α-limonene can be disproportionated to p-menthane and p-cymene over Pd and Pt catalysts on carrier materials. Also, Se-promoted PdO on a carrier material has been suggested as a catalyst [10]. Recently, Hölderich et al. reported a zeolite-supported Ce-promoted Pd catalyst for enhanced dehydrogenation activity during α-limonene conversion [11].

In this study, we have investigated the impact of zeolite structure upon shape selectivity in α-limonene conversion. Zeolites have been used in their acid form without the addition of Pd to avoid masking effects from the metal. To establish a relationship between zeolite structure and selectivity, we performed a modeling study on the diffusion behavior of the three cymene isomers in zeolite-Y and ZSM-5. These calculations have demonstrated the ability to provide valuable insights into the dynamical behavior of guest molecules in porous materials [12], allowing qualitative comparison of diffusion rates where thermodynamically controlled (the kinetic and entropic factors being inaccessible to the method). The predictions of the computational study are compared to the results of the reactor tests. This will indicate the value of these methodologies as predictive tools in future studies.

2. Methodology

2.1. Catalyst preparation

H-ZSM-5 zeolite with SiO_2/Al_2O_3 molar ratio of 55 and crystal size in the range of 3–5 μm was kindly provided by VAW Aluminum AG (AlSi-Penta-SH55). US-Y zeolite with SiO_2/Al_2O_3 molar ratio of 7.6 and crystal size in the range of 2–3 μm was kindly provided by PQ

© J.C. Baltzer AG, Science Publishers

Corp. (CBV760). The molecular sieve crystallinity was checked by X-ray diffraction and IR spectra of skeletal vibrations. Prior to their use the zeolites were shaped: zeolites were extruded into cords of 2 μm diameter, then dried overnight in air at 110 °C, calcined for 6 h in air at 550 °C and, finally, crushed into split of 1.0–1.6 mm.

2.2. α-limonene conversion

Catalytic activity tests were carried out in a fixed-bed down-flow stainless-steel integral reactor with a diameter of 6 mm at 200 and 300 °C and atmospheric pressure. 3.2 g of catalyst was used for each experimental run. α-limonene of 97% purity (3% other terpenes, kindly provided by Firmenich SA) was fed at a rate of 5 ml/h to the preheater, and reactant vapors were carried by a flow of 4 Nl/h N_2 to the catalyst bed. The resulting partial pressure in the feed was thus 16 kPa, WHSV was calculated to 1.3 h^{-1}. Online analysis of the products was done in a Siemens RGC 202 gas chromatograph, equipped with a 50 m OV 1701 CS column and a flame-ionization detector.

2.3. Simulations

The molecular mechanics calculations were carried out using the *Discover* simulation package [13], part of the *Solids_Diffusion* module of the *InsightII* program [14]. The potential parameters were taken from the consistent valence forcefield of Hagler et al. [15], shown in table 1. The non-bonded interaction potentials were of the Lennard-Jones form combined with a term describing the electrostatic interaction,

$$E_{\mathrm{nb}} = \sum_i \sum_{j>i} \left[\frac{A_{ij}}{r_{ij}^{12}} - \frac{B_{ij}}{r_{ij}^{6}} + \frac{q_i q_j}{r_{ij}} \right], \qquad (1)$$

where q_i and q_j are partial atomic charges, and the summation extends over all pairs of atoms i, j. Constants A_{ij} and B_{ij} are derived from atomic Lennard-Jones parameters using combination rules:

$$A_{ij} = (A_i A_j)^{1/2}; \qquad B_{ij} = (B_i B_j)^{1/2}. \qquad (2)$$

The intra-molecular interactions of the sorbate were described with regular bond length and bond angle expressions (table 1). During these calculations, the framework was held fixed at the energy-minimized geometry, with the exception of a 6 Å zone about the guest molecule, which was allowed to relax.

ZSM-5 has a two-dimensional intersecting pore system of sinusoidal and straight channels. The pores are approximately circular with a pore diameter of 5.5 Å. The zeolite-Y structure can be thought of as being made up of sodalite cages, fused through their six-ring faces (diameter 2.2 Å) by hexagonal prisms (double six-rings). This creates large spherical cavities, or supercages, of approximate diameter 13 Å. Access to the supercages is afforded by twelve-ring windows with a free aperture of 7.3 Å in diameter, which are tetrahedrally distributed around the center of the supercage. The cymene isomers are shown in figure 1. *p*-cymene has the smallest cross section of the three isomers.

Table 1
Potential parameters used in the diffusion path simulation: aromatic carbon (cp), sp^3-hybridized carbon (c), hydrogen (h), zeolite silicon (sz), and oxygen (oz). The non-bond interactions are calculated using combination rules.

Bond lengths: $E = k_i(r - r_0)^2$

Potential types		r_0 (Å)	k_1 (kcal mol^{-1} Å^{-2})
c	h	1.105	340.6175
cp	h	1.080	363.4164
cp	cp	1.340	480.0000
cp	c	1.510	283.0924
sz	oz	1.615	392.8000

Bond angles: $E = k_i(\theta - \theta_0)^2$

Potential types			r_0 (Å)	k_1 (kcal mol^{-1} Å^{-2})
h	c	h	106.4	39.5
h	c	c	110.0	44.4
cp	cp	h	120.0	37.0
cp	cp	cp	120.0	90.0
h	c	cp	110.0	44.4
c	cp	cp	120.0	44.2
cp	c	cp	110.5	46.6
sz	oz	sz	149.80	31.1
oz	sz	oz	109.47	100.3

Non-bonded interactions: $E = A_{ij}/r^{12} - B_{ij}/r^6$

Potential types	A (kcal mol^{-1} Å^{12})	B (kcal mol^{-1} Å^6)
h	7108.4660	32.87076
c	1981049.2250	1125.99800
cp	2968753.3590	1325.70810
sz	3149175.0000	710.00000
oz	272894.7846	498.87880

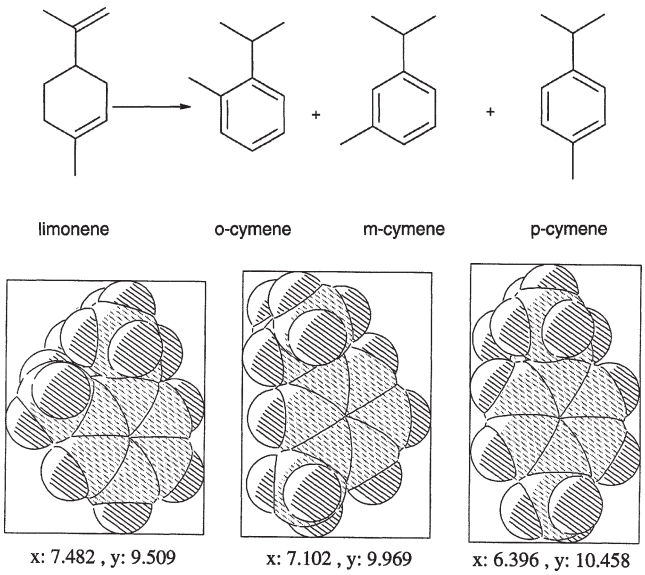

Figure 1. 2D depictions of limonene, and para-, ortho-, and meta-cymene. 3D structures and effective dimensions of the cymene isomers (in Å) are shown below. For a detailed description of the reaction mechanism and intermediates, see [8,9].

Table 2
Impact of zeolite structure on shape selectivity for ZSM-5 and zeolite-Y at 200 and 300 °C. WHSV is 1.3 h^{-1} and TOS is 0.5 h.

Zeolite	H-ZSM-5	US-Y	H-ZSM-5	US-Y
Temperature (°C)	200	200	300	300
α-limonene conversion (wt%)	87.8	99.5	99.2	100
Cym. selectivity (wt%)	11.7	22.3	18.1	7.7
Meta–para ratio	0.02	0.76	0.09	1.83

3. Results and discussion

3.1. Experimental

Shape selectivity of α-limonene conversion is strongly dependent upon zeolite structure, reaction temperature and time-on-stream (TOS). Table 2 presents m/p-cymene ratios for zeolite H-ZSM-5 and US-Y at 200 and 300 °C after 30 min on stream. Surprisingly, only traces of ortho-cymene were found at 30 min on stream over zeolite US-Y at 300 °C. No ortho-cymene was found over zeolite H-ZSM-5 and over US-Y at 200 °C. Similarly, it was unexpected that conversion over H-ZSM-5 did not yield any n-propyltoluenes, as observed by Parikh et al. [4], as a secondary reaction from p-cymene over MFI-type zeolites. The absence of n-propyltoluenes over US-Y-type zeolites is in line with observations by Wichterlova et al. [5] in the same temperature range during toluene alkylation.

Thus, a key indicator for shape selectivity during α-limonene conversion is the meta/para-cymene ratio in the product after short TOS. The m/p-cymene ratio of 1.83 over zeolite US-Y at 300 °C is close to the thermodynamic equilibrium value of 2.0, indicating very little shape-selective effects of the zeolite. The ratio is dropping to 0.76 for conversion at 200 °C. Assuming the pathway to meta-cymene via dealkylation of α-limonene and subsequent alkylation, a lower dealkylation rate necessarily leads to a lower m/p-cymene ratio. It is well known that cracking activity of acidic zeolites decreases at lower temperature. Thus, steric effects cannot be made responsible for the increase of shape selectivity at lower temperatures for both zeolite structures.

Conversion of α-limonene over H-ZSM-5 leads to very low values of the m/p-cymene ratio at 0.02 at 200 °C and 0.09 at 300 °C. This cannot be explained by a lower dealkylation rate, as toluene formation is dominant at short TOS. It can be concluded that steric constraints lead to drastically enhanced shape selectivity of MFI-type zeolites for α-limonene conversion. Shape-selective properties of ZSM-5 are well known and have been used commercially for various reactions as xylene isomerization before [16].

Generally, it is seen that with increasing TOS the m/p-cymene ratio is decreasing due to lower cracking activity, presumably due to coking of the acid sites. It is well known that the zeolites in the H-form yield toluene and propene/propane as cracking products [17]. In contrary to the use of acidic zeolites, the Na-ZSM-5 modified with Pd/Ce performs a much higher selectivity to p-cymene up to 90%. This has been published recently too [17].

3.2. Simulations

Inspection of the shapes of the three cymene isomers indicates that each isomer has a distinct cross section. This can lead to dramatic differences in diffusivity in zeolite channels, provided that the channels have appropriate dimensions. In principle, one could perform molecular dynamics calculations to calculate diffusion rates by evaluating the migration of the sorbates as a function of time. However, for large molecules, diffusion is too slow to be observed on a typical molecular dynamics time scale (100 ps). By making assumptions about the diffusion pathway, however, one can calculate the variation of the interaction energy along this pathway, which provides a measure on the relative diffusion barriers of different sorbates. This approach has proven to predict reliable trends in the diffusion properties of hydrocarbons in porous oxidic materials [12]. The sorbate is minimized at regular length intervals along the diffusion path, producing the "zero-kelvin" diffusion barrier. The diffusion path is defined by a pair of points at either side of the pore under investigation. The sorbate is iteratively moved along this defined trajectory. The sorbate is minimized with an harmonic potential applied which restraints the center of mass of the sorbate to a plane perpendicular to the trajectory. The restraint energy is subtracted at the end of the calculation. This procedure ensures that one obtains a minimum-energy path for diffusion along the channel.

A computational screening of diffusion properties of the o-, m-, and p-cymene isomers was carried out using this *biased diffusion* methodology [18]. The minimizations were carried out using periodic boundary conditions. This increases the accuracy of the interaction energies and allows one to simulate over shorter length scale, since edge effects are eliminated. For ZSM-5, we simulated diffusion through the straight channel, which is larger in diameter than the sinusoidal channel along the direction $\langle 0,1,0\rangle$. For zeolite-Y, the diffusion channel is made up of spherical cages and the twelve-ring windows connecting them. As a starting point, we chose the middle of the intersection of the straight pore and the unit cell, and we simulated for the length of the cell.

Since the diffusive behavior of molecules will most importantly be determined by the topology of the pore system, and only to a lesser degree by the presence of extra-framework particles such as metal clusters and extra-framework cations, we have performed the simulation on the silicious analogues of these zeolites, silicalite (ZSM-5) and faujasite, also for reasons of computational expediency. Also, because the majority of the interaction is with the framework oxygen, the strict Si/Al ordering is of less importance. The zeolite structural models were taken from the literature [19,20] and were then optimized using molecular mechanics, so their structures were consistent with the potential model and would introduce no artifacts due to

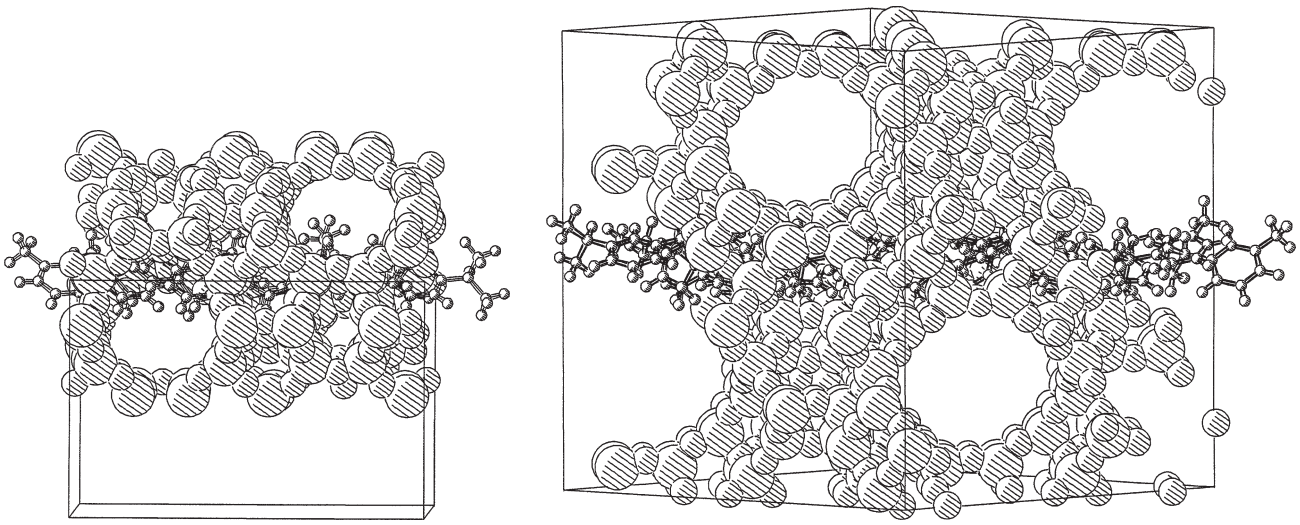

Figure 2. Diffusion profiles for meta-cymene in (a) ZSM-5 and (b) zeolite-Y.

residual strain. The pathways in both zeolites are depicted in figure 2, where snapshots of the diffusion trajectories of meta-cymene are shown.

Figure 3(a) shows the energy profiles for the diffusion of the three isomers in ZSM-5. The variation of the interaction energy between the host framework and the guest molecule provides information on the relative diffusion barriers of different guest molecules. It is evident that the diffusion of the para isomer is significantly less hindered than the diffusion of the ortho and meta isomers. The barriers for para diffusion are of the order of 30 kcal/mol, while the barriers for the meta and ortho isomers are 50 and 75 kcal/mol, respectively. These differences in diffusion barrier height will result in different life times of the molecule in the pore system, since there is a lower probability for crossing a higher energy barrier (relative rates cannot be given since the pre-exponential factors are unknown). The ortho and meta isomers are clearly obstructed in ZSM-5, but they seem to interact favorably with the zeolite between the activation barriers. This is in the channel intersections where the sorbates are less sterically hindered. This will allow conversion of these isomers when reacting on active sites on the inner surface of the pore system. If conversion leads to the para form, diffusion of the product is rapid, and it will be able to leave the pore system with the carrier gas. This can also rationalize the increase in the meta form with increasing temperature (table 2). While the low barrier for para diffusion is less affected by temperature, as it already has enough energy to surmount the barrier, the meta diffusion may increase because a higher temperature will increase the probability to overcome the diffusion barrier.

The diffusion profiles for the three isomers in zeolite-Y are different (figure 3(b)). There is no significant diffusion barrier for any of the isomers. Isomerization of cymenes will not result in changes in diffusivity of the gas, and it is expected that the reaction will lead to equal proportions of the three isomers. This supports the experimental finding that this zeolite shows no noticeable selectivity for the reaction.

The incorporation of framework relaxation does not affect the observed trends in this study, but does affect the value of the calculated binding energies. This is especially notable in the case of o-cymene/ZSM-5, where it amounts to some 6 kcal/mol. Little relaxation was observed for the zeolite-Y case, indicative of the greater rigidity of this structure, and the lower energy barriers, hence strain.

Besides differences in diffusion rates, there might be other factors that enhance selectivity. The reaction from limonene to cymene itself may be influenced by steric constraints imposed by the zeolite framework. The transition state for the conversion to o- and m-cymenes is likely to be more "bent" than the transition states for the para-isomer. These bent transition states would be less favorable in the smaller channels and will also increase the selectivity for the para isomer. In the abscence of such steric hindrance, e.g., in the gas phase, a greater probability for these "strained" transition states may exist. These reactions will preferably take place at the pore intersections, as there is more room to accommodate a bulky transition state. Since both zeolite-Y and ZSM-5 have a three-dimensional connected pore structure, it is expected that transition-state selectivity, as discussed here, is of less importance than in one-dimensional zeolitic frameworks as, e.g., zeolite-L or mordenite.

4. Conclusions

α-limonene can be dehydrogenated to p-cymene, but care has to be taken to avoid secondary reactions and rapid deactivation of the catalyst due to coke deposition. Employing a medium-pore HZSM-5 zeolite or NaZSM-5 avoids transalkylation of p-cymene, as observed for large-pore zeolite support.

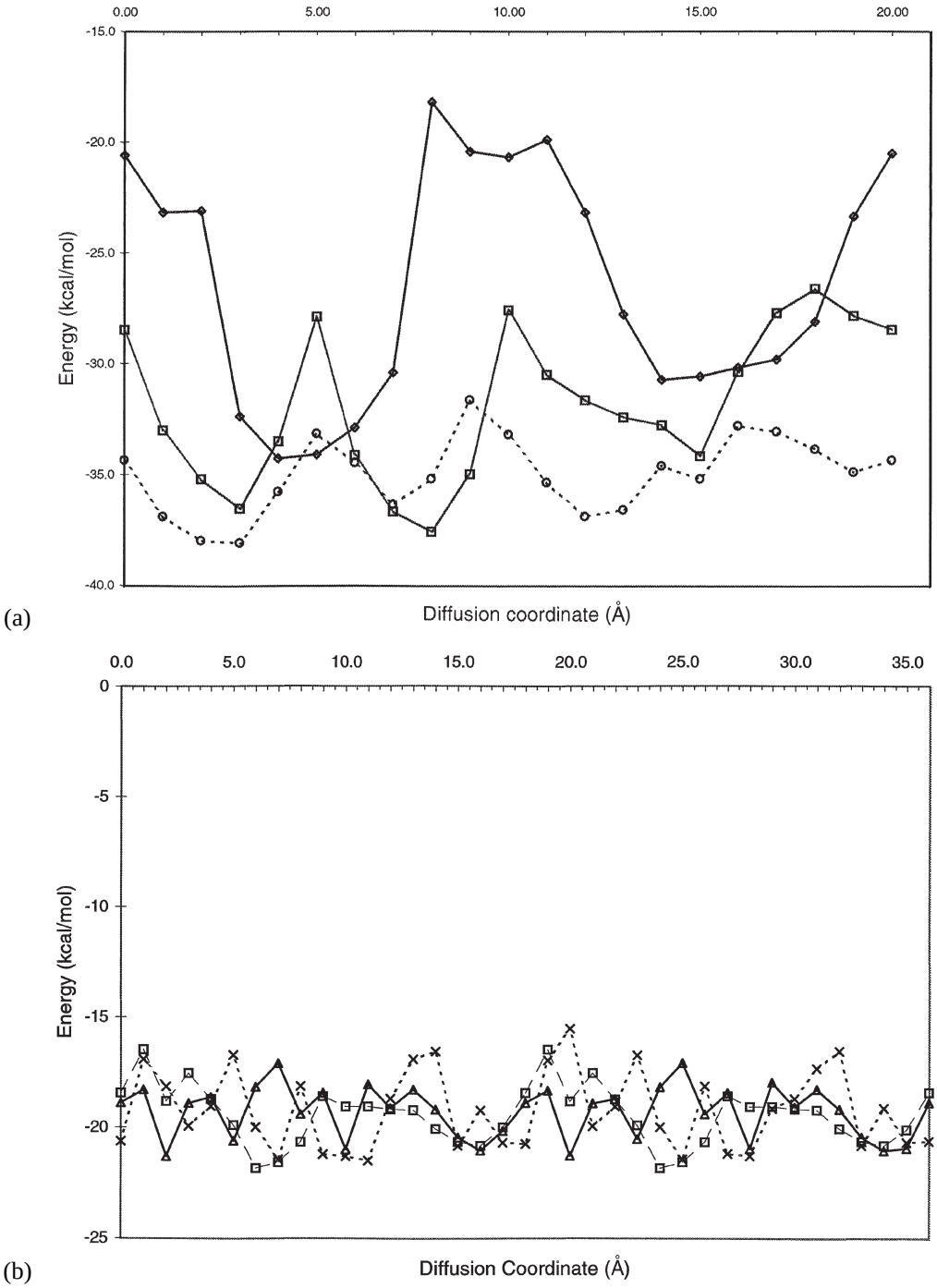

Figure 3. Energy profiles for diffusion for ortho- (△), meta- (×), and para-cymene (□) in (a) ZSM-5 and (b) zeolite-Y. ZSM-5 clearly exhibits differences in diffusion properties for the three isomers.

Molecular mechanics calculations confirm the experimental findings that ZSM-5 performs the hydrogenation selectively to produce preferentially *p*-cymene and provide a precise atomistic explanation for these observations. Zeolite-Y is predicted to have no selectivity towards any of the cymene isomers, also in agreement with the experiments. The good agreement between experiments and modeling confirms the reliability of molecular modeling methods in the screening of zeolites for shape-selective reactions.

References

[1] J.M. Derfer and M.M. Derfer, in: *Kirk–Othmer Encyclopedia of Chemical Technology*, Vol. 22 (1978) p. 709.
[2] W.J. Welstead, Jr., in: *Kirk–Othmer Encyclopedia of Chemical Technology*, Vol. 9 (1978) p. 544.
[3] K. Ito, in: *Kirk–Othmer Encyclopedia of Chemical Technology* (1973) p. 89.
[4] P.A. Parikh, N. Subrahmanyam, Y.S. Bhat and A.B. Halgeri, Chem. Eng. J. 54 (1994) 79.
[5] B. Wichterlova, A. Kapustin and J. Cejka, Appl. Catal. A 108 (1994) 187.

[6] J. Das, Y.S. Bhat and A.B. Halgeri, Catal. Lett. 32 (1995) 319.
[7] P.A. Parikh, N. Subrahmanyam, Y.S. Bhat and A.B. Halgeri, Appl. Catal. A 90 (1992) 1.
[8] J. Zelinski, Ber. 57 (1924) 2058.
[9] R.P. Linstead, K.O. Michaelis and S.L.S. Thomas, J. Chem. Soc. (1940) 1139.
[10] R. Martin and W. Gramlich, Patents DE 36 07 448 and US 4 720 603 (1987).
[11] W.F. Hölderich, W.D. Mross, R. Fischer and F.-F. Pape, Patents DE 3 513 569 (1986), US 4 665 252 (1987) and EP 0199 209 (1988).
[12] J.A. Horsley, J.D. Fellmann, E.G. Derouane and C.M. Freeman, J. Catal. 147 (1994) 231.
[13] *Discover 4.0.0* (Molecular Simulations, Inc., San Diego, CA).
[14] *InsightII 4.0.0* (Molecular Simulations, Inc., San Diego, CA).
[15] A.T. Hagler, S. Lifson and P. Dauber, J. Am. Chem. Soc. 101 (1979) 5122.
[16] J. Wie, J. Catal. 76 (1982) 433.
[17] P.A. Weyrich and W.F. Hölderich, J. Appl. Catal. (1997), in press.
[18] S.D. Pickett, A.K. Nowak and J.M. Thomas, Zeolites 9 (1989) 123.
[19] D.H. Olson, J. Phys. Chem. 74 (1970) 2758.
[20] H. van Koningsveld, H. van Bekkum and J.C. Jansen, Acta Crystallogr. B 43 (1987) 127.